

NAGW-665
NAG 2-329

HQ 6RPM
7N-91-CR

(NASA-CR-186147) DISSOCIATIVE RECOMBINATION
IN AERONOMY (State Univ. of New York) 22 p

N90-70551

3

Unclass

00/91 0252403

DISSOCIATIVE RECOMBINATION IN AERONOMY

J. L. Fox

Institute for Atmospheric Sciences
and
Department of Mechanical Engineering
State University of New York at Stony Brook
Stony Brook, NY 11794

AAAI/IS

1988 DEC -5 A 8:23

RECEIVED
LIBRARY

ABSTRACT

The importance of dissociative recombination in planetary aeronomy is summarized and two examples are discussed. The first is the role of dissociative recombination of N_2^+ in the escape of nitrogen from Mars. A previous model is updated to reflect new experimental data on the electronic states of N produced in this process. Second, the intensity of the atomic oxygen green line on the nightside of Venus is modeled. Use is made of theoretical rate coefficients for production of $O(^1S)$ in dissociative recombination from different vibrational levels of O_2^+ .

1. INTRODUCTION

Dissociative recombination (DR) is an important elementary process in planetary upper atmospheres for several reasons. Its obvious importance is to the ionization structure: it provides a loss mechanism for molecular ions that is unavailable to atomic ions. Consequently molecular ions have shorter chemical lifetimes at high altitudes than atomic ions. The relative importance of dissociative recombination compared to ion-neutral reactions depends on the availability of the latter. Ion-neutral reactions tend to transform ions into other ions whose parent neutrals have lower ionization potentials. This is strictly true for charge transfer reactions and is practically true for other ion-neutral reactions because the dissociation energies of atmospheric molecules tend not to differ as much as ionization potentials. Generally, for ions derived from parent neutrals with low ionization potentials, dissociative recombination may be the major loss process over a wide range of altitudes. For those derived from neutrals with high ionization potentials, dissociative recombination may dominate at sufficiently high altitudes. In the terrestrial ionosphere, for example, the most important molecular ions are N_2^+ , O_2^+ and NO^+ . For N_2^+ , whose parent N_2 has a relatively high ionization potential of 15.58 eV, DR is the most important loss mechanism only above 250 km.

Immediately below that altitude, the major loss process is reaction with O:



O_2 has an intermediate ionization potential of 12.15 eV, and DR controls the loss of O_2^+ over a larger altitude range, beginning at about 190 km. The reaction



is the most important loss mechanism immediately below that altitude. NO has the lowest ionization potential of any of the major atmospheric species and consequently DR of NO^+ is the only loss mechanism available over the entire ionosphere.

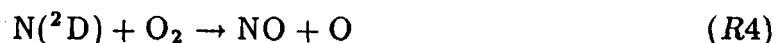
Dissociative recombination may be an important source of airglow emissions, if the fragments are produced in excited states with short radiative lifetimes. In DR of CO_2^+ ,



55% of the CO molecules are produced in the excited $\text{CO}(a^3\Pi)$ state.¹⁾ $\text{CO}(a^3\Pi)$ is a metastable state with a lifetime of about 8 ms^{2,3)}; it radiates to the ground $^1\Sigma$ state producing emission in the well-known Cameron Band System. The Cameron Bands are the brightest features in the ultra-violet dayglows of Venus and Mars. On Venus, approximately 5 kR of 20 kR total integrated intensity is due to DR of CO_2^+ .⁴⁾ (One kiloRayleigh (kR) is an apparent column emission rate of 10^9 photons $\text{cm}^{-2}\text{s}^{-1}$.) In DR of O_2^+ , the O atoms may be produced in various combinations of the electronic states 3P , 1D , and 1S . $\text{O}(^1D)$ radiates to the ground state producing the 6300 Å "red line" and $\text{O}(^1S)$ to $\text{O}(^1D)$ producing the 5577 Å "green line". This source is important in the dayglows and nightglows of all the terrestrial planets and in terrestrial auroras. It is relatively more important in the nightglow, due to the absence of sources involving the direct interaction of solar radiation or photoelectrons with atmospheric gases.

The fragments produced in dissociative recombination may be important chemically. For example, ionization of N_2 followed by dissociative recombination of N_2^+ is a net source of odd nitrogen, an important family of species that are interconverted more rapidly than they are created or destroyed. The fragments may also be formed in metastable excited states whose chemistry is different from that of ground state species. For example, in DR of $\text{N}_2^+(v=0)$, the yield of $\text{N}(^2D)$

has recently been measured by Queffelec et al. to be about 1.85.⁵⁾ $N(^2D)$ may radiate to the ground $N(^4S)$ state, producing emission at 5200 Å, but the transition probability is small, about $1.06 \times 10^{-5} \text{ s}^{-1}$.⁶⁾ It is probable that the atom will be chemically destroyed before radiating. In the terrestrial atmosphere, the reaction



is an important source of NO,^{7,8)} as is the reaction



on Venus and Mars.^{9,10)} Reactions of ground state N atoms with O_2 and CO_2 are much slower than reactions (R4) and (R5).^{11,12,13,14)} Constantinides et al.¹⁵⁾ have shown that the reaction



which is endothermic for ground state N atoms, is the most important source of N^+ above 250 km in the terrestrial ionosphere.

That the fragments produced in dissociative recombination may have large kinetic energies has several important consequences for planetary atmospheres. First, DR may be an important heat source for the neutral atmosphere. On Earth, most of the heating due to exothermic reactions is from dissociative recombination reactions.¹⁶⁾ On Venus, DR of O_2^+ is the dominant heat source above 135 km.¹⁷⁾ If the fragments are produced at a sufficiently high altitude and with sufficient kinetic energy, they may escape from the planet. (See the review by Hunten¹⁸⁾ for a description of thermal and non-thermal escape processes.) A common approximation, is that above the *exobase*, where the mean free path is equal to a scale height, the atmosphere is assumed to be collisionless. Then all atoms traveling upward with velocities greater than the escape velocity actually escape. For thermal escape, this approximation has been shown to produce essentially no error.¹⁹⁾ The cut-off velocity, v_{esc} is that for which the kinetic energy, $\frac{1}{2}mv^2$, is equal to the gravitational potential energy, mgr , where r is the distance of the exobase from the center of the planet. On Mars, the escape velocity is about 5 km/s, corresponding to an escape energy of 0.125 eV per amu. DR of O_2^+ , CO^+ and N_2^+ are sufficiently exothermic in at least some channels to produce escaping O, C and N atoms. On Venus and Earth the escape energies exceed 0.5 eV per amu and none of the dissociative recombination processes are exothermic enough

to produce escaping atoms. On Venus, dissociative recombination is implicated in an indirect way in the escape of H through the sequence²⁰⁾



followed by the transfer of energy in a collision of the translationally hot O^* with an H atom:



Cooper et al.²¹⁾ have computed the fraction of H atoms that come away from (R8) with energy greater than the escape energy as 6.9 and 8.5% at 200 and 300 K, respectively.

Even if the atoms released above the exobase have insufficient energy to escape, they may travel to high altitudes producing a "corona" of hot atoms surrounding the planet. The hot O coronas of the terrestrial planets are produced mainly by the dissociative recombination of O_2^+ at the exobase. The hot O corona of the Earth has been discussed Yee et al.²²⁾ Such a corona was predicted for Venus and Mars by Wallis²³⁾ and distributions of hot O have been computed by Nagy et al.,²⁴⁾ Paxton,²⁵⁾ and Nagy and Cravens.²⁶⁾ The hot C corona around Venus has been studied by analysis of the limb profiles of the atomic carbon emission multiplets at 1561 and 1657 Å measured by the Pioneer Venus Orbiter (PVO) Ultraviolet Spectrometer.²⁵⁾ These features are produced at high altitudes by fluorescent scattering of sunlight by atomic carbon. The hot C is produced partly in dissociative recombination of CO^+ , but mostly by (R7) followed by



a process that Paxton refers to as "sputtering", but which is more accurately termed "knock-on"¹⁸⁾

In the remainder of this article, two problems in planetary aeronomy in which dissociative recombination plays a major role will be described in detail. The first is the escape of nitrogen from Mars. In modeling this phenomenon, knowledge of the kinetic energies and therefore, indirectly, the electronic states of the N atoms produced in DR of N_2^+ is important. Second, the production of the atomic oxygen green line in the nightglow of Venus is discussed. Here the production rates of $\text{O}(^1S)$ from dissociative recombination of O_2^+ in different vibrational levels is required.

2. THE ESCAPE OF NITROGEN FROM MARS

The mass spectrometer on the Viking spacecraft measured an anomalous $^{15}\text{N} : ^{14}\text{N}$ ratio of about 0.0060 in the Martian atmosphere; the value in the terrestrial atmosphere is 0.00368.^{27,28)} This isotope enhancement of a factor of 1.62 over the terrestrial value is presumably due to preferential escape of ^{14}N . The thermosphere of Mars is composed mostly of CO_2 , with smaller amounts of N_2 , O , CO , Ar , O_2 and NO . The model thermosphere used here is essentially the same as that used by Fox and Dalgarno²⁹⁾ and the calculations described here are an updating of that model. At the *turbopause* (about 120 km), the mixing ratio of N_2 is about 2.5%.³⁰⁾ Diffusion largely controls the distribution of species above the turbopause, so the mixing ratios of heavier species decrease with altitude and those of lighter species increase. Thus between the turbopause and the exobase at about 200 km, the ratio, f of $^{15}\text{N}^{14}\text{N} : ^{14}\text{N}_2$ decreases. The exact value of the ratio at the exobase, f_c depends on the ratio at the turbopause, f_o , which is assumed equal to that in the bulk atmosphere, and on the value of the eddy diffusion coefficient, a measure of the strength of mixing in the thermosphere. McElroy et al.³¹⁾ computed the deficiency factor $R = f_c/f_o$ and reported a value of about 0.82. If we call $\phi(t)$ the $^{14}\text{N}_2$ flux at time t , \mathcal{N}_{14} the column density of $^{14}\text{N}_2$ and \mathcal{N}_{15} the column density of $^{15}\text{N}^{14}\text{N}$ then

$$\frac{d\mathcal{N}_{14}}{dt} = -\phi(t) \quad (1)$$

and

$$\frac{d\mathcal{N}_{15}}{dt} = -f_c\phi(t) = -Rf\phi. \quad (2)$$

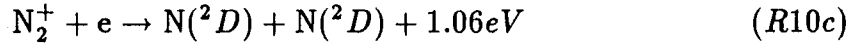
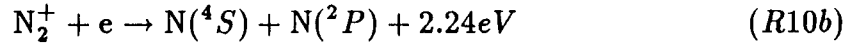
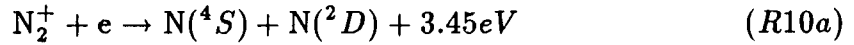
Combining (1) and (2) we obtain an equation for the isotope ratio f :²⁷⁾

$$\frac{df}{dt} = \frac{\phi f(1 - R)}{\mathcal{N}_{14}}. \quad (3)$$

The isotope enhancement produced by escape operating over a time t before the present can be obtained by integrating equation (3) backward in time. The effects on the escape rate of changes in the composition of the atmosphere and in the heights of the exobase and turbopause are taken into account as described by Fox and Dalgarno.²⁹⁾

The steady state ion densities are computed by solving the continuity equations including photochemistry and ambipolar diffusion and the results are shown

in Fig. 1. Also shown are the O_2^+ and CO_2^+ densities derived from the Viking I Retarding Potential Analyzer and reported by Hanson et al.³²⁾ The atomic oxygen density was not measured by the mass spectrometers and has been adjusted to fit the O_2^+ and CO_2^+ densities at the ion peak. A mixing ratio of 2% at about 130 km is derived. The N_2^+ density peaks above the exobase at approximately 215 km where it attains a value of about 180 cm^{-3} . The total rate of N_2^+ DR above the exobase is about $2 \times 10^6 \text{ cm}^{-2} \text{ s}^{-1}$, but not all channels are sufficiently exothermic for escape to occur. Dissociative recombination may produce N atoms in three channels:



Because the N escape energy is 1.74 eV, escape is possible only when the reaction proceeds via (R10a). If a statistical distribution of products is assumed, the fraction of dissociative recombinations proceeding by (R10a) is about 0.24. With this assumption, DR is the dominant N escape mechanism.^{29,33)} The measurements of Queffelec et al.⁵⁾ have shown, however, that the predominant channel is (R10c) and that the yield of $N(^4S)$ is less than 0.10. We therefore assume that an upper limit to the fraction of dissociative recombinations proceeding according to (R10a) is 0.10.

For most escape mechanisms, preferential escape of ^{14}N is assumed to occur only because the ratio $^{15}\text{N}^{14}\text{N} : ^{14}\text{N}_2$ is reduced at the exobase compared to that in the bulk atmosphere. The process of dissociative recombination via channel (R10a) itself, however, discriminates against ^{15}N . The escape energy of ^{14}N is about half the exothermicity of (R10a), but the escape energy of ^{15}N is 1.86 eV, much more than half the energy released. Wallis²³⁾ computed the escape probabilities for both atoms and found that ^{14}N is about twice as likely to escape as ^{15}N . The exothermicities shown for (R10a-c) apply to DR of N_2^+ ions in the ground vibrational state. For vibrationally excited ions, the exothermicity is larger and the isotope discrimination due to the mechanism itself disappears! In order to model the evolution of the isotope ratio, it is necessary to determine the fraction of dissociative recombinations that occur from vibrationally excited states. Therefore we need to know the vibrational distribution of N_2^+ at the exobase and the rate

Table 1. The vibrational distribution of N_2^+ at the Martian exobase, 200 km.

v	Fraction
0	0.56
1	0.21
2	0.107
3	0.058
4	0.035
5	0.028

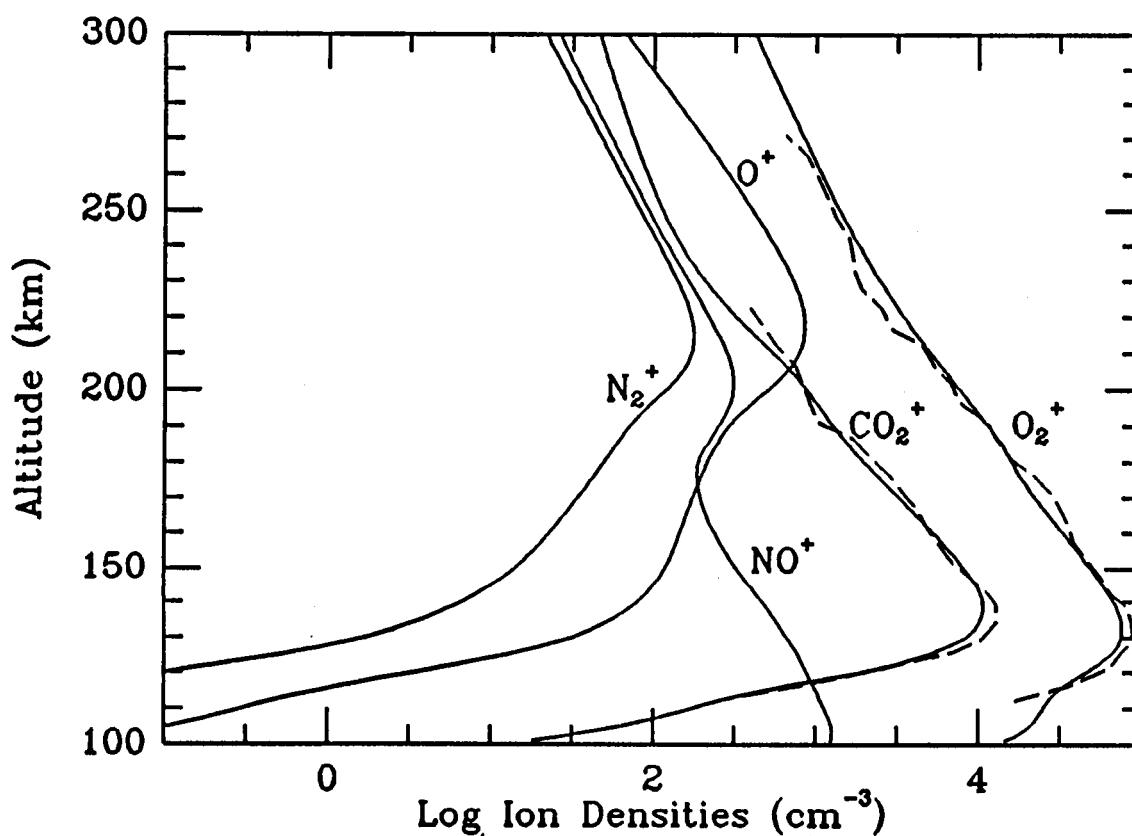
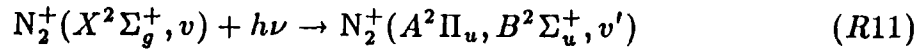
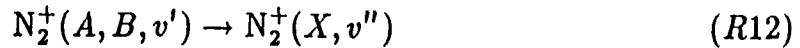


Fig. 1. Altitude profiles of the steady state ion densities for low solar activity. The solar zenith angle is 60° . The dashed lines are Viking 1 data from Hanson et al. (Ref. 32).

coefficients for dissociative recombination from individual vibrational levels. The latter are not available, although evidence suggests that the rate coefficient increases with increasing vibrational level.³⁴⁾ We adopt the rate coefficient reported by Zipf³⁴⁾ of $2.2 \times 10^{-7} (300/T_e)^{0.39} \text{ cm}^3 \text{ s}^{-1}$ for dissociative recombination from all the vibrational levels ($v = 0 - 5$) included in the calculation. The model of Fox and Dalgarno²⁹⁾ for the vibrational distribution of N_2^+ at the exobase on Mars has been updated (c.f. Fox and Dalgarno³⁵⁾) and the distribution presented in Table 1 was computed. The vibrational distribution at the exobase is essentially controlled by fluorescent scattering of sunlight in the Meinel and First Negative Band systems, which can be represented by

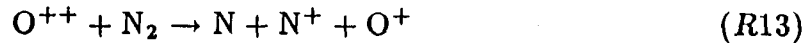


followed by



The fraction of N_2^+ ions in vibrationally excited levels is found to be about 44%, so the isotope discrimination operates only 56% of the time.

The ^{14}N escape fluxes from all sources are presented in Table 2. Values for both high and low solar activity were computed and averaged to obtain the escape fluxes used in the calculation. The values for photodissociation, photodissociative ionization, and photoelectron impact ionization are unchanged from those of Fox and Dalgarno.²⁹⁾ The products of the reaction



are unknown, but exothermicity is large, about 10.9 eV, and it is assumed that an energetic N atom is produced in every reaction. The reaction



produces an N atom in the 2D state at least 90% of the time.³⁶⁾ In that case the exothermicity is not sufficient to allow escape of the N atom produced. We assume initially that 10% of the reactions (R1) produce a ground state N atom. With these assumptions, dissociative recombination is still the largest source of escaping N atoms, but photodissociation and reaction (R1) are comparable. The differential escape of ^{15}N and ^{14}N due to DR from the ground vibrational level,

Table 2. ^{14}N Escape Fluxes ($10^4\text{cm}^{-2}\text{s}^{-1}$)

Process	Solar Activity		
	Low	High	Average
$\text{N}_2 + h\nu \rightarrow \text{N} + \text{N}$	5.9	14	10
$\text{N}_2 + h\nu \rightarrow \text{N}^+ + \text{N} + \text{e}$	1.7	6.0	3.9
$\text{N}_2 + \text{e} \rightarrow \text{N}^+ + \text{N} + 2\text{e}$	1.4	4.8	3.1
$\text{N}_2^+ + \text{O} \rightarrow \text{NO}^+ + \text{N}$	6.1	17	11
$\text{O}^{++} + \text{N}_2 \rightarrow \text{N}^+ + \text{N} + \text{O}^+$	0.6	1.7	1.1
$\text{N}_2^+ + \text{e} \rightarrow \text{N} + \text{N}$	4.0	22	13
TOTAL	20	66	42

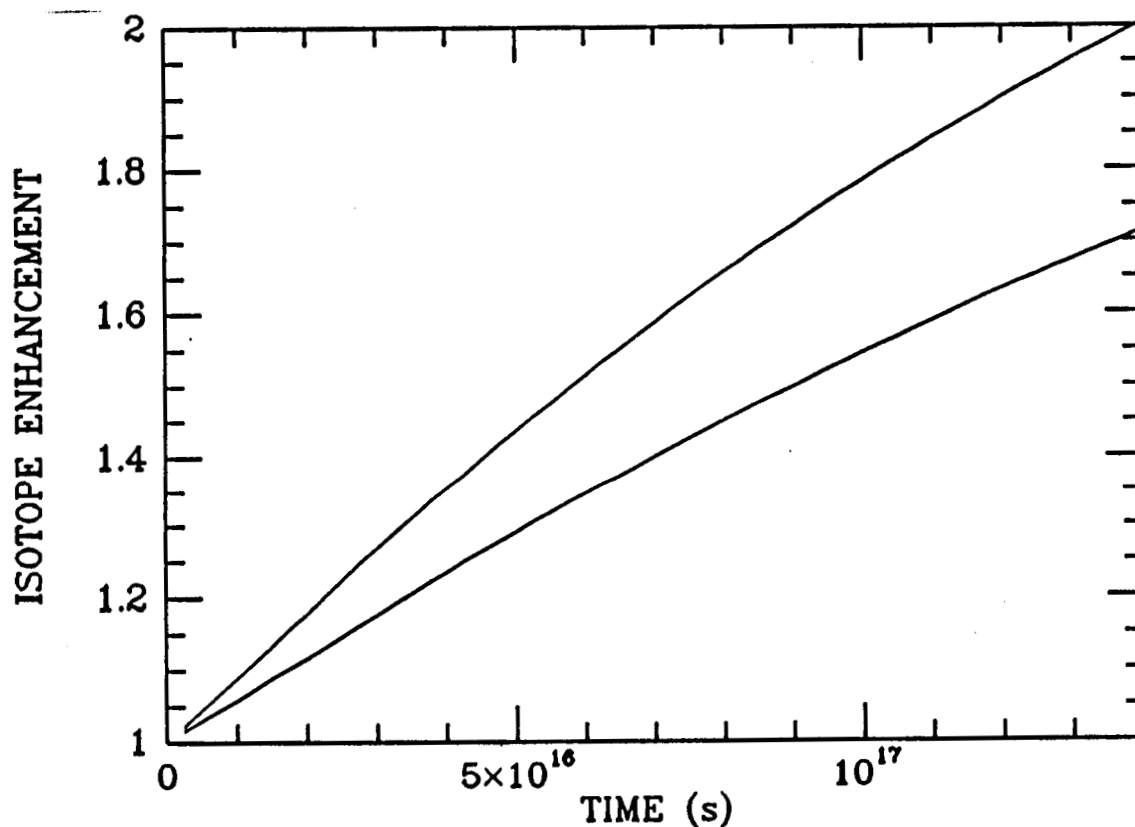


Fig. 2. Evolution of the isotope enhancement, the ratio $^{15}\text{N}:^{14}\text{N}$ relative to the terrestrial value. The upper curve was calculated assuming fluxes due to (R1) and (R10) equal to their upper limits, as explained in the text. The lower curve is for both fluxes reduced by half.

however, causes this mechanism to produce a much larger isotope enhancement than the other mechanisms.

Using the average escape fluxes shown in Table 2 and integrating equations (1) and (3) backward in time over the age of the solar system, 4.6×10^9 years (1.45×10^{17} s), we find an initial column density of 8.5×10^{22} N₂ molecules cm⁻², about 14 times that found in the present atmosphere. The resulting isotope enhancement is shown in Fig. 2. The isotope enhancement for the escape processes operating over 4.6×10^9 years is 2.0, somewhat larger than the measured value. An isotope enhancement of 1.62 is reached in 7.5×10^{16} s (2.4×10^9 years). The escape fluxes due to reaction (R1) and to dissociative recombination are actually upper limits, so we tested the sensitivity of the model to the assumed yields by reducing both fluxes by half. The resulting initial N₂ column density is reduced by one-third and the predicted isotope enhancement is 1.71. The difference between the measured and the model isotope enhancements is probably within the uncertainties in the model. The magnitude of the solar flux, for example, in the early solar system was undoubtedly different from the current values, but arguments have been presented for both larger^{37,38)} and smaller values.³⁹⁾ The isotope enhancement predicted for a statistical distribution of product states in (R10) was much larger, about 2.51.²⁹⁾ It was necessary then to invoke a mechanism to reduce the escape fluxes in the past, such as a denser CO₂ atmosphere, surviving over a period exceeding 2×10^9 years. Such an atmosphere has been predicted (e.g. Cess et al.⁴⁰⁾, Pollack et al.⁴¹⁾) to be consistent with an earlier presence of liquid water on the surface. While it is no longer necessary, a dense CO₂ atmosphere is not excluded by the current model, as long as it was lost early in the history of the solar system.

3. THE GREEN LINE OF ATOMIC OXYGEN ON THE NIGHTSIDE OF VENUS

Ultra-violet emission features of atomic oxygen at 1304 and 1356 Å have been seen on the nightside of Venus by the PVO Ultraviolet Spectrometer.⁴²⁾ Fox and Stewart⁴³⁾ have suggested that the emissions are due to the precipitation of soft electrons into the nightside atmosphere. Suprathermal electrons have been detected outside the atmosphere by the PVO Retarding Potential Analyzer⁴⁴⁾ and by the plasma analyzers on the Soviet spacecraft Veneras 9 and 10.⁴⁵⁾ The PVO measurements suggest that the electron energy spectrum approximates a Maxwellian distribution with a characteristic energy of about 14 eV. Impact of such electrons

should also excite atomic oxygen to the 1S and 1D states, producing emission at 5577 and 6300 Å. The Venera 9 and 10 fly-by spacecraft carried visible spectrophotometers, but no 5577 Å emission was measured on the nightside of Venus and an upper limit of 10 R has been placed on its intensity⁴⁶⁾ (Krasnopol'sky, private communication, 1985). This upper limit places another constraint on models for the auroral production mechanism. In order to evaluate the constraint, it is necessary to predict the rate of production of the green line from other sources. Dissociative recombination of O_2^+ (R7) is probably the most important source in the nightglow. The production of $O(^1S)$ in (R7) has been shown to depend on the vibrational quantum number of O_2^+ . Abreu et al.⁴⁷⁾ showed that the 5577 Å emission in the terrestrial nightglow depends on the ratio of the electron density to atomic oxygen density, a measure of the extent of vibrational excitation of O_2^+ .⁴⁸⁾ Guberman^{49,50)} has performed *ab initio* calculations of the rate coefficients for the production of $O(^1S)$ and $O(^1D)$ in DR from the lower vibrational levels of O_2^+ . He has shown in particular that the rate coefficient for production of $O(^1S)$ is a strong function of vibrational level, increasing almost 2 orders of magnitude from $v = 0$ to $v = 2$. We have constructed a model of the nightside ionosphere of Venus, including a model of the vibrational distribution of O_2^+ , and we have used Guberman's rate coefficients to predict the intensities of the red and green lines in the Venus nightglow.

The thermosphere of Venus is similar to that of Mars, and consists mostly of CO_2 at low altitudes, with small amounts of N_2 , CO and O . The neutral densities we have used are taken from the model of Hedin et al.⁵¹⁾ for 165° solar zenith angle and $F_{10.7} = 200$. This model is based on measurements of the PVO Neutral Mass Spectrometer.⁵²⁾ The nightside ionosphere is maintained largely by transport of atomic ions, primarily O^+ , from the dayside ionosphere.^{53,54)} Cravens et al.⁵⁵⁾ constructed a quasi-two-dimensional model that showed that the observed O^+ horizontal velocities from the dayside are sufficient to maintain the nightside ionosphere. Spenner et al.⁵⁶⁾ showed that a flux of O^+ ions of $1 - 2 \times 10^8 \text{ cm}^{-2} \text{ s}^{-1}$ over the nightside is sufficient to maintain the observed mean ion densities. The nightside ionosphere is, however, highly variable and almost always exhibits some degree of disturbance.^{57,58)} Sometimes the ionosphere disappears completely, leaving only a few scattered patches of plasma.⁵⁹⁾ Our model ionosphere is designed to represent "full-up" relatively undisturbed conditions, when we expect the rate

of DR to be substantial, although not necessarily a maximum. We have modeled this ionosphere by introducing a flux of O^+ of $1.0 \times 10^8 \text{ cm}^{-2} \text{ s}^{-1}$ at the top of our model thermosphere. Fluxes of other atomic ions, including C^+ , N^+ and O^{++} were assumed proportional to their densities at high altitudes on the nightside as measured by the PVO Ion Mass Spectrometer.⁶⁰⁾ Altitude profiles of the major ions in the resulting ionosphere are shown in Fig. 3. The effect of drag on the upward diffusion of molecular ions by the downward flux of O^+ is included in an approximate way by reducing the diffusion coefficients of the molecular ions by a factor of 10. This factor was chosen to reproduce the approximate shape of the measured O_2^+ profiles presented by Taylor et al.⁶⁰⁾ The maximum O_2^+ density in our model is about $2.4 \times 10^4 \text{ cm}^{-3}$.

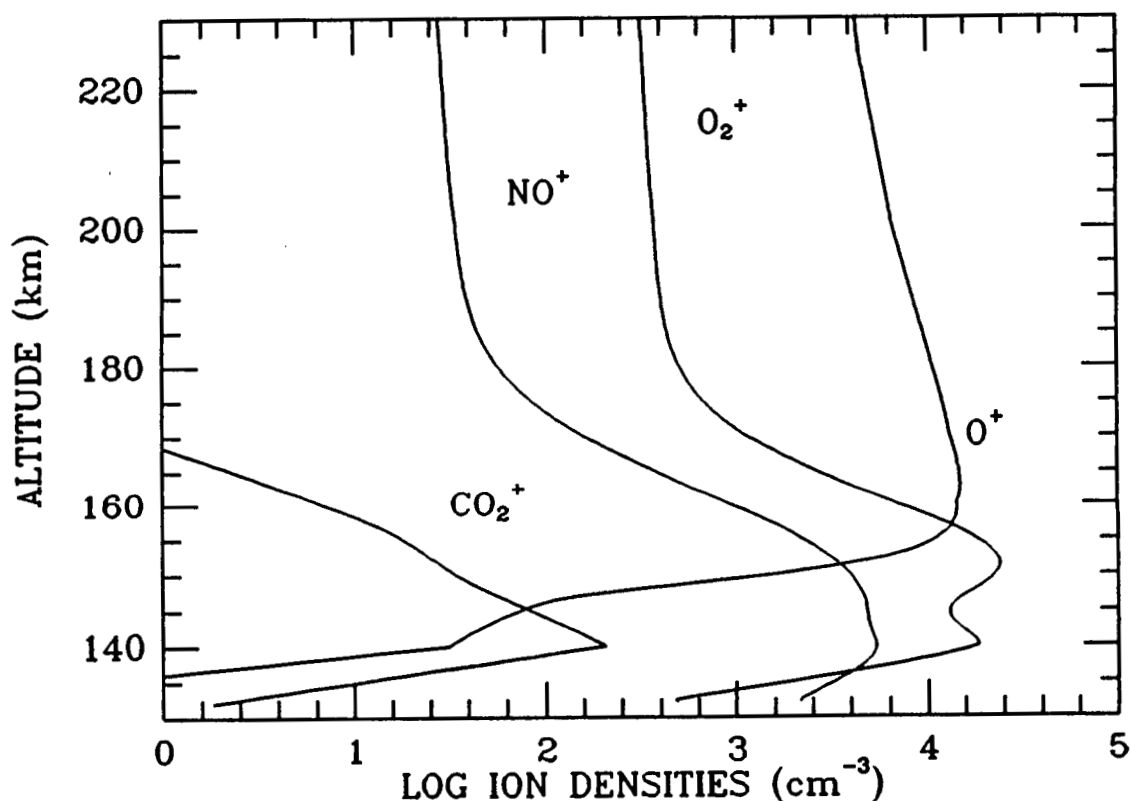
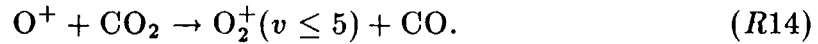
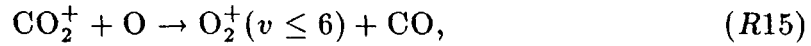


Fig. 3. Computed profiles for the major ion densities in the nightside ionosphere of Venus. The model was constructed by introducing a flux of O^+ of $1.0 \times 10^8 \text{ cm}^{-2} \text{ s}^{-1}$ at the top of the neutral atmosphere.

Vibrationally excited $O_2^+(v)$ is produced on the nightside mainly in the reaction



The rate coefficient for this reaction is large, about $9.4 \times 10^{-10} \text{ cm}^3 \text{ s}^{-1}$.⁶¹⁾ In the dayside ionosphere, the major source of O_2^+ is



which has a rate coefficient $k = 1.64 \times 10^{-10} \text{ cm}^3 \text{ s}^{-1}$.⁶²⁾ The nascent vibrational distribution produced in these reactions is unknown, so the energetically accessible vibrational levels are assumed to be populated equally. Since the distribution assumed for the production reactions is similar, and fluorescent scattering is not important for O_2^+ , we expect the steady state vibrational distribution on the nightside to be similar to that computed for the dayside.⁶³⁾ Loss of O_2^+ is mostly by DR, reaction (R7), but in the lower ionosphere reactions with N

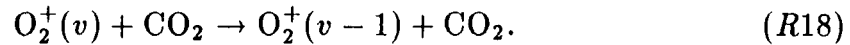


and NO

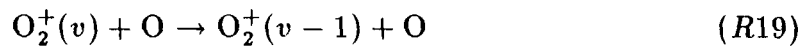


are also important.

In addition to the net sources and sinks of O_2^+ , there are mechanisms that interchange vibrational levels with no net production or loss. Quenching of vibrational excitation is one such mechanism. In the lower ionosphere, the most important quencher is CO_2 :

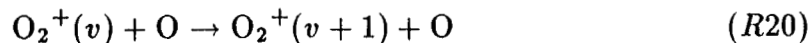


The rate coefficient for this reaction is surprisingly large, about $1-2 \times 10^{-10} \text{ cm}^3 \text{ s}^{-1}$. The rate coefficients for this and other quenching reactions have been taken from the measurements of Böhringer et al.⁶⁴⁾ The rate coefficient for quenching by atomic oxygen



is unknown, but is probably large. We assume first a rate coefficient of $1 \times 10^{-10} \text{ cm}^3 \text{ s}^{-1}$, but we test the sensitivity of the model to this rate coefficient by

repeating the calculations with a nearly gas kinetic value of $6 \times 10^{-10} \text{ cm}^3 \text{ s}^{-1}$.
Collisional excitation



is the reverse of quenching and the rate coefficient is related to that for quenching by detailed balance, that is, $k_{20} = k_{19} \times e^{-\Delta E/kT}$, where ΔE is the energy difference between the vibrational levels.

We have solved the continuity equations for O_2^+ , taking into account vibrational levels $v = 0-60$ of the ground electronic state, as was done for the dayside⁶³⁾ and for the Earth.⁶⁵⁾ Fig. 4 shows the fractions of O_2^+ in the first four vibrational levels as a function of altitude from 130 km to 200 km. The calculation of the

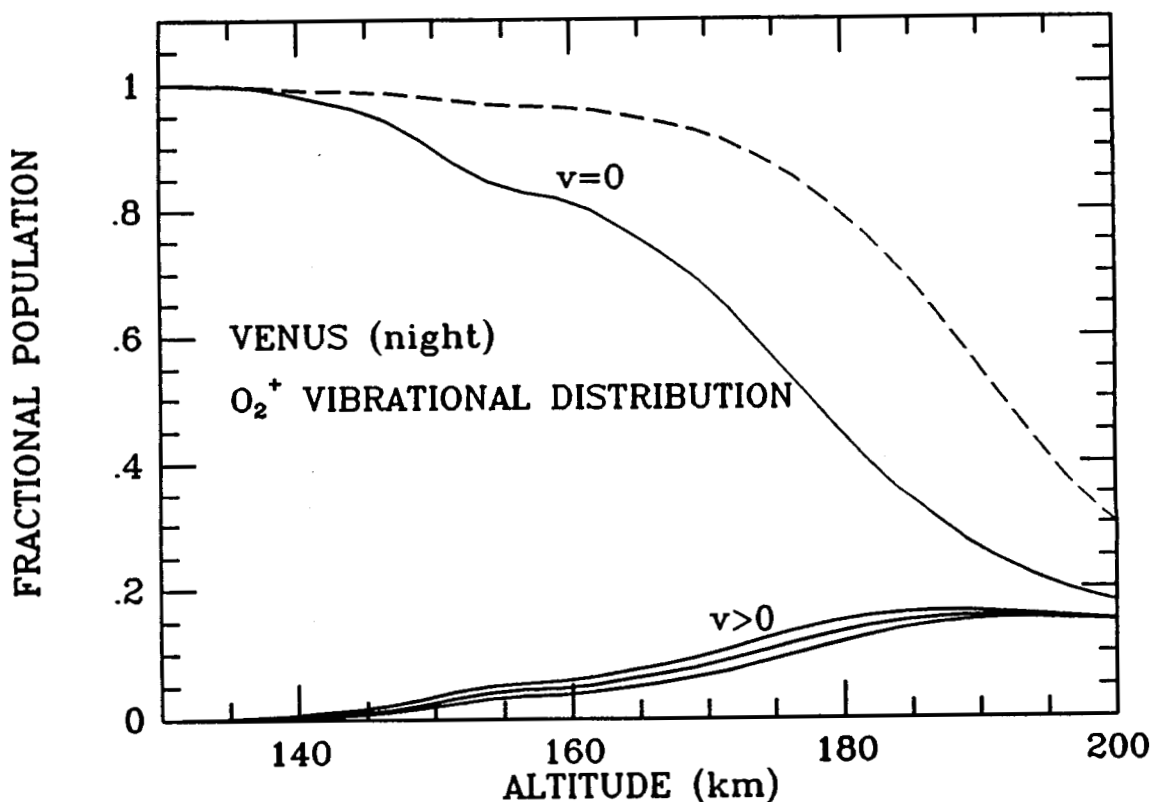


Fig. 4. Fractions of O_2^+ ions in vibrational states $v = 0 - 3$ as a function of altitude calculated with a photochemical steady state model, with an assumed value for k_{19} of $1 \times 10^{-10} \text{ cm}^3 \text{ s}^{-1}$. The curves labeled $v > 0$ are, from top to bottom, $v = 1$, $v = 2$ and $v = 3$. The dashed line is the fraction in $v = 0$ for $k_{19} = 6 \times 10^{-10} \text{ cm}^3 \text{ s}^{-1}$.

steady state ion densities includes transport by ambipolar diffusion, but the calculation of the vibrational distribution assumes photochemical equilibrium. Consequently, the distributions shown in Fig. 4 are probably valid only below about 170 km. The ions at higher altitudes are produced largely by transport from below. The dashed line shows the fraction in $v = 0$ for the larger rate coefficient for (R19), $k_{19} = 6 \times 10^{-10} \text{cm}^3 \text{s}^{-1}$. It should be noted here that the number of vibrational quanta lost in (R19) is unknown and may be more than the assumed value of 1, because the reaction can occur by atom-interchange,⁴⁸⁾ but the rate coefficient and the average number of vibrational quanta lost cannot be varied independently in a meaningful way.

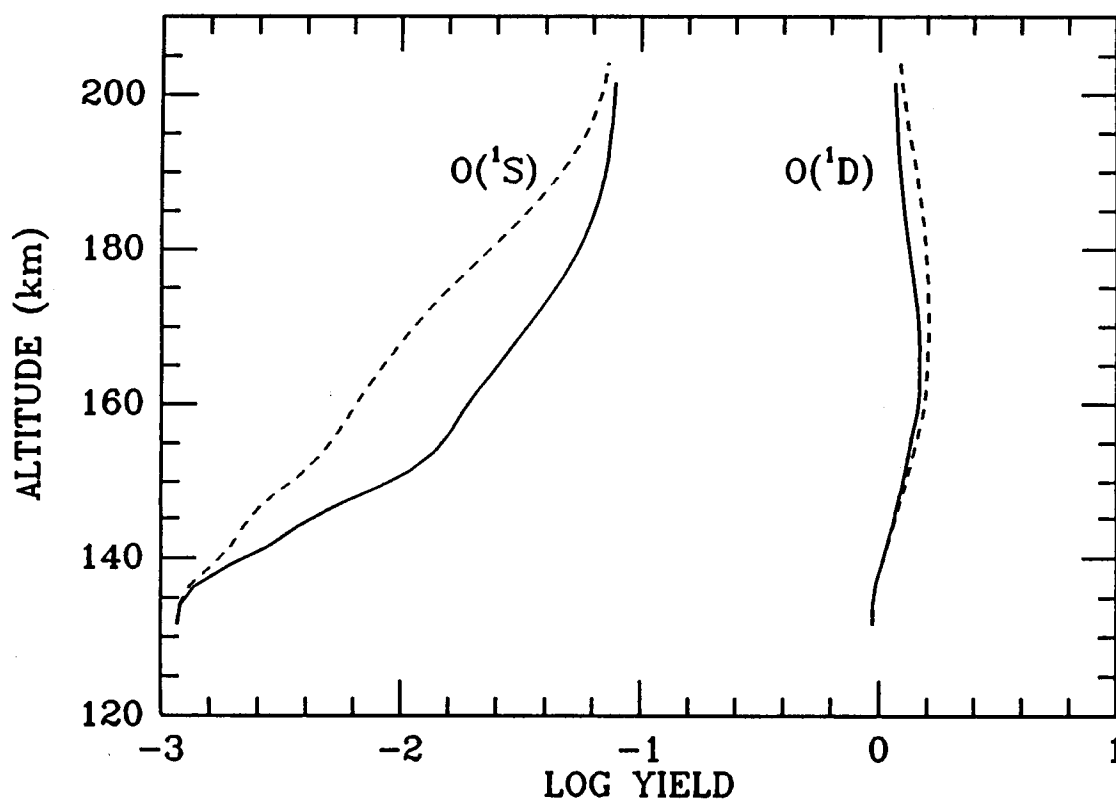


Fig. 5. Altitude profiles of the yields of $\text{O}(^1S)$ and $\text{O}(^1D)$ produced in dissociative recombination of $\text{O}_2^+(v)$. Solid lines are computed assuming $k_{19} = 1 \times 10^{-10} \text{cm}^3 \text{s}^{-1}$. Dashed lines are for $k_{19} = 6 \times 10^{-10} \text{cm}^3 \text{s}^{-1}$.

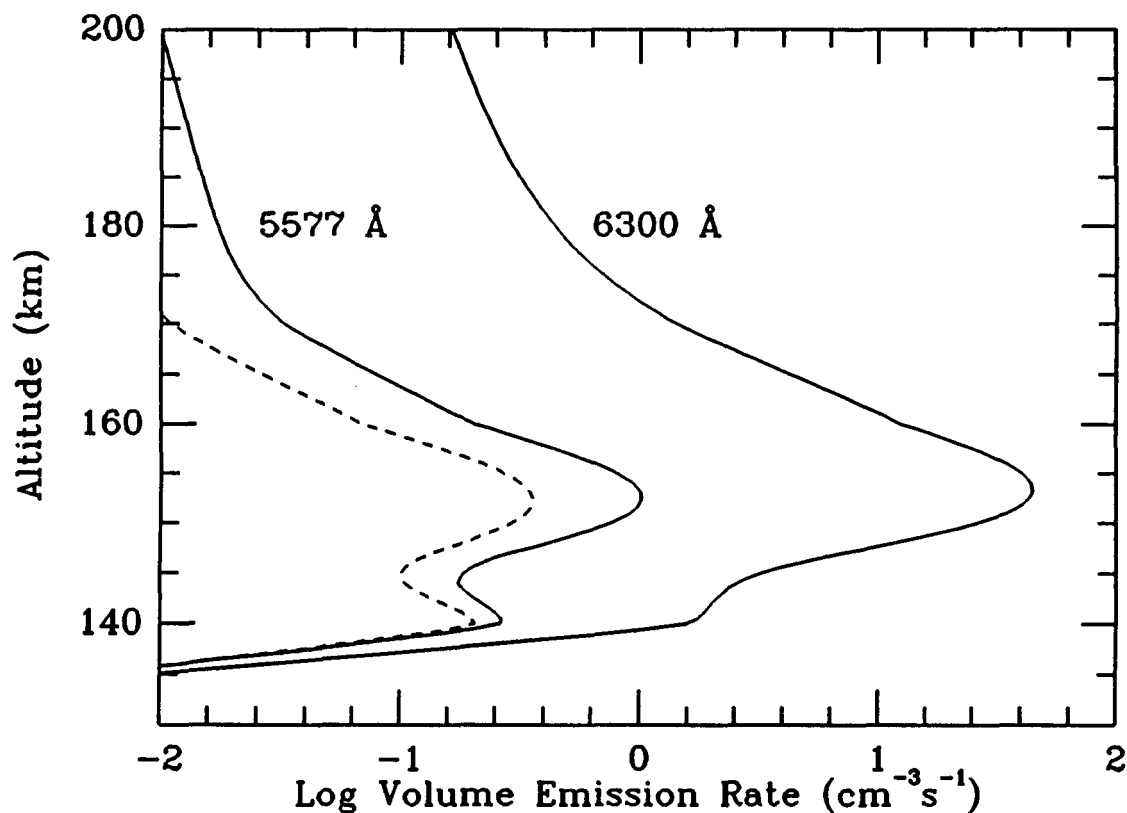


Fig. 6. Altitude profiles of the volume emission rates of the red and green lines of atomic O. Solid lines are computed assuming $k_{19} = 1 \times 10^{-10} \text{ cm}^3 \text{ s}^{-1}$. The dashed line is for $k_{19} = 6 \times 10^{-10} \text{ cm}^3 \text{ s}^{-1}$.

The vibrational distributions are combined with the rate coefficients from Guberman^{49,50}) and the total DR rate coefficient from Alge et al.⁶⁶) to give the yields for $\text{O}(^1S)$ and $\text{O}(^1D)$. For dissociative recombination from vibrational levels for which no information is available, the rate coefficient is assumed to be equal to that for the highest level for which data are available. Altitude profiles of the yields and the volume emission rates are shown in Figs. 5 and 6, respectively. The $\text{O}(^1S)$ yield varies from much less than 1% to about 8% at high altitudes. Fig. 6 shows that most of the emission arises between 140 and 160 km where the 1S yield is in the range 1 – 2%. The dashed lines show the yields and volume emission rates for the assumption of the larger value for k_{19} . The integrated overhead intensities are 1.2R for the green line and 46R for the red line. If O_2^+ is quenched by O at the larger rate, the integrated green line intensity is reduced to

0.5 R. Since the maximum electron density is somewhat larger than the average nightside value⁵⁸⁾ the upper limit for auroral production is probably close to the measured upper limit. Had we adopted a yield of, say, 10% for the production of $O(^1S)$, independent of vibrational level of O_2^+ , as has been done often in the past, close to 10 R would be predicted from dissociative recombination alone. A flux of soft electrons of sufficient magnitude to produce the observed 1304 and 1356 Å intensities produces 4 to 7 R of 5577 Å emission.⁴³⁾ The results of this study of the green line show that the auroral model remains viable.

Acknowledgements

This work has been supported in part by grant ATM 8700436 from the National Science Foundation to the Massachusetts Institute of Technology and by grants NAGW-665 and NAG2-329 from the National Aeronautics and Space Administration to the Research Foundation of the State University of New York at Stony Brook.

REFERENCES

1. Wauchop, T. S. and H. P. Broida, Lifetime and quenching of $\text{CO}(a^3\Pi)$ produced by recombination of CO_2 ions in a helium afterglow. *J. Chem. Phys.*, **56**, 330 (1972).
2. James, T. C., Transition moments, Franck-Condon factors, and lifetimes of forbidden transitions. Calculation of the intensity of the Cameron system of CO, *J. Chem. Phys.* **55**, 4118 (1971).
3. Lawrence, G. M., Quenching and radiation rates of $\text{CO}(a^3\Pi)$, *Chem. Phys. Lett.* **9**, 575 (1971).
4. Fox, J. L. and A. Dalgarno, Ionization, luminosity and heating of the upper atmosphere of Venus, *J. Geophys. Res.* **86**, 629 (1981).
5. Queffelec, J. L., B. R. Rowe, M. Morlais, J. C. Gomet and F. Vallee, The dissociative recombination of $\text{N}_2^+(v = 0, 1)$ as a source of metastable atoms in planetary atmospheres, *Planet. Space Sci.* **33**, 263 (1985).
6. Garstang, R. H., Transition probabilities of auroral lines, in *The Airglow and Aurorae*, ed. by E. B. Armstrong and A. Dalgarno, p. 324, Pergamon, New York (1956).
7. Cravens, T. E., J. C. Gérard, A. I. Stewart and D. W. Rusch, The latitudinal gradient of nitric oxide in the thermosphere. *J. Geophys. Res.* **84**, 2675 (1979).
8. McCoy, R. P., Thermospheric odd nitrogen 1. NO, $\text{N}(^4S)$ and $\text{O}(^3P)$ densities from rocket measurements of the NO δ and γ bands and the O_2 Herzberg I bands. *J. Geophys. Res.* **88**, 3197 (1983).
9. Rusch, D. W. and T. E. Cravens, A model of the neutral and ion chemistry in the daytime thermosphere of Venus. *Geophys. Res. Lett.* **6**, 791 (1979).
10. Fox, J. L., The chemistry of metastable species in the Venusian ionosphere, *Icarus* **61**, 248, (1982).
11. Lin, C. L. and F. Kaufman, Reactions of metastable nitrogen atoms, *J. Chem. Phys.* **55**, 3760 (1971).
12. Baulch, D. L., D. D. Drysdale, D. G. Horne and A. C. Lloyd, *Evaluated Kinetic Data for High Temperature Reactions. II. Homogeneous Gas Phase Reactions of the $\text{H}_2\text{-N}_2\text{-O}_2$ System*, Butterworths, London (1973).
13. Brown, R. and C. A. Winkler, The chemical behavior of active nitrogen. *Angew. Chem. intern. Edit.* **9**, 181 (1970).
14. Piper, L. G., M. E. Donahue and W. T. Rawlins, Rate coefficients for $\text{N}(^2D)$

- reactions *J. Phys. Chem.* 91, 3883 (1987).
15. Constantinides, E. R., J. H. Black, A. Dalgarno and J. H. Hoffman, The Photochemistry of N^+ ions. *Geophys. Res. Lett.* 6, 569 (1979).
 16. Torr, M. R., P. G. Richards and D. G. Torr, A new determination of the ultraviolet heating efficiency of the thermosphere. *J. Geophys. Res.* 85, 6819 (1980).
 17. Fox, J. L., Heating efficiencies in the thermosphere of Venus reconsidered, *Planet. Space Sci.* 36, 27 (1988).
 18. Hunten, D. M., Thermal and non-thermal escape mechanisms for terrestrial bodies, *Planet. Space Sci.* 30, 773 (1982).
 19. Chamberlain, J. W., Planetary coronae and atmospheric evaporation, *Planet. Space Sci.* 11, 901 (1963).
 20. McElroy, M. B., M. J. Prather and J. M. Rodriguez, Escape of hydrogen from Venus, *Science*, 215, 614 (1982).
 21. Cooper, D. L., J. H. Yee, and A. Dalgarno, Energy transfer in oxygen-hydrogen collisions, *Planet. Space Sci.* 32, 825 (1984).
 22. Yee, J. H., J. W. Meriwether, P. B. Hays, Detection of a corona of fast oxygen atoms during solar maximum, *J. Geophys. Res.* 85, 3396 (1980).
 23. Wallis, M. K., Exospheric density and escape fluxes of atomic isotopes on Venus and Mars, *Planet. Space Sci.* 26, 949 (1978).
 24. Nagy, A. F., T. E. Cravens, J.-H. Yee and A. I. F. Stewart, Hot atoms in the upper atmosphere of Venus, *Geophys. Res. Lett.* 8, 629 (1981).
 25. Paxton, L. J., Atomic carbon in the Venus thermosphere: observations and theory, *PhD thesis*, University of Colorado (1983).
 26. Nagy, A. F. and T. E. Cravens, Hot oxygen atoms in the upper atmospheres of Venus and Mars, *Geophys. Res. Lett.* 15, 933 (1988).
 27. Nier, A. O., M. B. McElroy and Y. L. Yung, Isotopic composition of the Martian atmosphere. *Science* 194, 68, (1976).
 28. Nier, A. O. and M. B. McElroy, Composition and structure of Mars upper atmosphere: Results from the neutral mass spectrometers on Viking 1 and 2, *J. Geophys. Res.* 82, 4341 (1977).
 29. Fox, J. L. and A. Dalgarno, The escape of nitrogen from Mars, *J. Geophys. Res.*, 88, 9027 (1983).
 30. Nier, A. O., W. B. Hanson, A. Seiff and M. B. McElroy, Composition and struc-

- ture of the Martian atmosphere: Preliminary results from Viking I. *Science* 193, 786 (1976).
31. McElroy, M. B., T. Y. Kong and Y. L. Yung, Photochemistry and evolution of Mars atmosphere: a Viking perspective, *J. Geophys. Res.* 82, 4379 (1977).
 32. Hanson, W. B., S. Sanatani and D. R. Zuccaro, The Martian ionosphere as observed by the retarding potential analyzers, *J. Geophys. Res.* 82, 4351 (1977).
 33. Fox, J. L. and A. Dalgarno, The production of nitrogen atoms on Mars and their escape, *Planet. Space Sci.* 28, 41 (1980).
 34. Zipf, E. C., The dissociative recombination of vibrationally excited N_2^+ ions. *Geophys. Res. Lett.* 7, 645 (1980).
 35. Fox, J. L. and A. Dalgarno, The vibrational distribution of N_2^+ in the terrestrial ionosphere, *J. Geophys. Res.* 90, 7557 (1985).
 36. Frederick, J. E., and D. W. Rusch, On the chemistry of metastable atomic nitrogen in the *F* region deduced from simultaneous satellite measurements of the 5200-Å airglow and atmospheric composition, *J. Geophys. Res.* 82, 3509 (1977).
 37. Canuto, V. M., J. S. Levine, T. R. Augustson and C. L. Imhoff, UV radiation from the young sun and oxygen and ozone levels in the prebiological palaeoatmosphere, *Nature* 296, 816 (1982).
 38. Zahnle, K. J. and J. C. G. Walker, The evolution of solar ultraviolet luminosity, *Rev. Geophys. Space Phys.* 20, 280 (1982).
 39. Newman, M. J. and R. T. Rood, Implications of solar evolution for the Earth's early atmosphere, *Science* 198, 1035 (1977).
 40. Cess, R. D., V. Ramanathan and T. Owen, The Martian paleoclimate and enhanced atmospheric carbon dioxide, *Icarus* 41, 159 (1980).
 41. Pollack, J. B., F. J. Kasting, S. M. Richardson and K. Poliakoff, The case for a wet, warm climate on early Mars, *Icarus* 71, 201 (1987).
 42. Phillips, J. L., A. I. F. Stewart and J. G. Luhmann, The Venus ultraviolet aurora: observations at 130.4 nm, *Geophys. Res. Lett.* 13, 1047 (1986).
 43. Fox, J. L. and A. I. F. Stewart, The Venus ultraviolet aurora: a soft electron source, *in preparation* (1988).
 44. Knudsen, W. C. and K. L. Miller, Pioneer Venus superthermal electron flux measurements in the Venus umbra, *J. Geophys. Res.* 90, 2695 (1985).

45. Gringauz, K. I., M. I. Verigin, T. K. Breus, and T. Gombosi, The interaction of electrons in the optical umbra of Venus with the planetary atmosphere—The origin of the nighttime ionosphere. *J. Geophys. Res.* 84, 2123 (1979).
46. Krasnopolsky, V. A., Excitation of oxygen emissions in the night airglow of the terrestrial planets, *Planet. Space Sci.* 29, 925 (1981).
47. Abreu, V. J., R. W. Eastes, J. H. Yee, S. C. Solomon and S. Chakrabarti, Ultraviolet nightglow production near the magnetic equator by neutral particle precipitation, *J. Geophys. Res.* 91, 11,365 (1986).
48. Bates, D. R. and E. C. Zipf, The $O(^1S)$ quantum yield of O_2^+ dissociative recombination, *Planet. Space Sci.* 28, 1081 (1980).
49. Guberman, S. L., The production of $O(^1D)$ from dissociative recombination of O_2^+ , *Planet. Space Sci.* 36, 47 (1988).
50. Guberman, S. L., The production of $O(^1S)$ in dissociative recombination of O_2^+ , *Nature*, 327, 408 (1987).
51. Hedin, A. E., H. B. Niemann, W. T. Kasprzak and A. Seiff, Global empirical model of the Venus thermosphere, *J. Geophys. Res.* 88, 73 (1983).
52. Niemann, H. B., W. T. Kasprzak, A. E. Hedin, D. M. Hunten and N. W. Spencer, Mass spectrometric measurements of the neutral gas composition of the thermosphere and exosphere of Venus, *J. Geophys. Res.* 85, 7817 (1980).
53. Knudsen, W. C., K. Spenner, K. L. Miller and V. Novak, Transport of ionospheric O^+ ions across the Venus terminator and implications, *J. Geophys. Res.* 85, 7803 (1980).
54. Knudsen, W. C., K. Spenner, and K. L. Miller, Antisolar acceleration of ionospheric plasma across the Venus terminator. *Geophys. Res. Lett.* 8, 241 (1981).
55. Cravens, T. E., S. L. Crawford, A. F. Nagy and T. I. Gombosi, A two-dimensional model of the ionosphere of Venus, *J. Geophys. Res.* 88, 5595 (1983).
56. Spenner, K., W. C. Knudsen, R. C. Whitten, P. F. Michelson, K. L. Miller and V. Novak, On the maintenance of the Venus nightside ionosphere: electron precipitation and plasma transport, *J. Geophys. Res.* 86, 9170 (1981).
57. Taylor, H. A., R. E. Hartle, H. B. Niemann, L. H. Brace, R. E. Daniell, S. J. Bauer and A. J. Kliore, Observed composition of the ionosphere of Venus: implications for the ionization peak and the maintenance of the nightside ionosphere.

- sphere, *Icarus* 51, 283 (1982).
58. Knudsen, W. C., K. L. Miller and K. Spenner, Median density profiles of the major ions in the central nightside Venus ionosphere. *J. Geophys. Res.* 91, 11,936 (1986).
 59. Cravens, T. E., L. H. Brace, H. A. Taylor, C. T. Russell, W. L. Knudsen, K. L. Miller, A. Barnes, J. D. Mihalov, F. L. Scarf, S. J. Quenon and A. F. Nagy, Disappearing ionospheres on the nightside of Venus. *Icarus* 51, 271 (1982).
 60. Taylor, H. A., H. C. Brinton, S. J. Bauer, R. E. Hartle, P. A. Cloutier and R. E. Daniell, Global observations of the composition and dynamics of the ionosphere of Venus: implications for the solar wind interaction. *J. Geophys. Res.* 85, 7765 (1980).
 61. Smith, D., N. G. Adams and T. M. Miller, A laboratory study of the reactions of N^+ , N_2^+ , N_3^+ , N_4^+ , O^+ , O_2^+ and NO^+ with several molecules at 300 K, *J. Chem. Phys.* 69, 308 (1978).
 62. Fehsenfeld, F. C., D. B. Dunkin and E. E. Ferguson, Rate constants for the reaction of CO_2^+ with O, O_2 and NO; N_2^+ with O and NO; and O_2^+ with NO. *Planet. Space Sci.* 18, 1267 (1970).
 63. Fox, J. L., The O_2^+ vibrational distribution in the Venusian ionosphere, *Adv. Space Res.* 5, 165 (1985).
 64. Böhringer, H., M. Durup-Ferguson, E. E. Ferguson and D. W. Fahey, Collisional vibrational quenching of $O_2^+(v)$ and other molecular ions in planetary atmospheres, *Planet. Space Sci.*, 31, 483 (1983).
 65. Fox, J. L., The O_2^+ vibrational distribution in the dayside ionosphere, *Planet. Space Sci.* 34, 1252 (1986).
 66. Alge, E., N. G. Adams and D. Smith, Measurements of the dissociative recombination coefficients of O_2^+ , NO^+ and NH_4^+ in the temperature range 200 – 600 K. *J. Phys. B.* 16, 1433 (1983).